

Research Article

A Novel Compact CP Antenna with Wide Axial Ratio Bandwidth for Worldwide UHF RFID Handheld Reader

Waleed Abdelrahim Ahmed  and Feng Quanyuan 

School of Information Science and Technology, Southwest Jiaotong University, Chengdu 611756, China

Correspondence should be addressed to Feng Quanyuan; fengquanyuan@163.com

Received 20 January 2019; Revised 18 February 2019; Accepted 3 March 2019; Published 2 May 2019

Academic Editor: Ikmo Park

Copyright © 2019 Waleed Abdelrahim and Feng Quanyuan. This is an open access article distributed under the Creative Commons Attribution License, which permits unrestricted use, distribution, and reproduction in any medium, provided the original work is properly cited.

This study presents a novel compact circularly polarized antenna for universal ultrahigh-frequency (UHF) radio-frequency identification (RFID) handheld reader applications. The antenna is composed of a coplanar waveguide (CPW) L-shaped feedline mounted at the right edge of the square slot at the bottom of the ground plane to realize a circular polarization; a horizontal stub protruded from the right side of the square slot towards the slot centre, and a vertical stub is mounted at the lower left of the square slot. The designed antenna printed on one ground plane layer of a low-cost FR4 substrate with an overall size of $120 \times 120 \times 1.6 \text{ mm}^3$. The measurement results show indicate that the fabricated antenna achieves a wide axial ratio (AR) bandwidth of 460 MHz (818–1278 MHz), wide impedance bandwidth of 54.6% (630–1103 MHz), and a measured peak gain of 4.0 dBi. The proposed antenna is a good candidate for compact universal UHF RFID handheld reader applications (840–960 MHz).

1. Introduction

Radio-frequency identification (RFID) is an auto-ID technology that uses radio-frequency waves for the purpose of tracking and identifying objects in supply chains, access control, warehouses, commerce, and so on [1, 2]. Compared to other kinds of identification technologies, RFID has been receiving much attention due to its advantages, such as a high data transfer rate, longer information storage capability, and high reliability. RFID technology can be categorized into four categories according to its use in different frequency bands, namely, low-frequency (LF), high-frequency (HF), ultrahigh-frequency (UHF), and microwave RFID systems. Recently, RFID systems, especially in the global UHF band from 840 to 960 MHz (13.3%), have gained popularity due to the advantages of high data transfer rate, fast reading speed, and long detection range [3, 4].

Basically, the RFID system comprises an RFID tag (tag antenna+an application-specific integrated circuit (ASIC)), an RFID reader device (reader with its antenna), and a host computer for the purpose of information processing. Briefly,

the reader sends a radio-frequency signal to the RFID tag antenna using an antenna and receives a modulated signal back from the tag. To receive the radio-frequency signal from the reader antenna, the RFID tag must be into the reading zone of the reader antenna [5].

In practical usage, the UHF RFID tag antennas usually are linearly polarized (LP) and the UHF RFID tags are normally oriented arbitrarily. To ensure the reliability of the communications between RFID reader devices and RFID tags, a reader antenna with a circularly polarized (CP) characteristic is highly required [6]. The reader antenna for RFID systems are one of the most significant parts of the RFID systems. Sometimes, their inability to accommodate new operating scenarios can restrict the RFID system performance as a whole. UHF RFID handheld reader applications require a compact antenna with low profile and light weight.

Over the past years, several CP reader antennas such as microstrip antennas [7, 8], patch antennas [9, 10], and stacked-architecture antennas [11, 12] that were designed with various techniques to operate in the UHF RFID range

have been investigated. However, the aforementioned RFID reader antennas [7–12] are unable to cover the global UHF RFID band (840 MHz to 960 MHz) owing to their narrow impedance and axial ratio (AR) bandwidths, relatively large sizes, and incompatibility with a handheld reader or application which needs to have a small-sized antenna.

Some reader antennas demonstrate a big gain, but their sizes are too large to use in handheld reader applications. Compact antennas that have simple structures, inexpensive, and easy to fabricate are tremendously needed for UHF RFID handheld reader applications. Subsequently, lowering the fabrication cost of the RFID reader antennas and simplifying their design are an interesting target for many researchers and manufacturers in this field. For RFID system implementation and cost reduction, designing a universal reader antenna with acceptable performance throughout the universal UHF RFID range would be beneficial. Slot antennas have the merits of a small size, easy to design, an inexpensive, and wide frequency bandwidth. In recent years, two similar CP slot antennas have been presented, such as the planar broadband antenna with a square slot and F-shaped feedline to operate in the UHF RFID band in [13] and wideband universal CP reader antenna with a circular slot and fed by a coplanar waveguide (CPW) L-shaped feedline in [14]. However, both antennas have a relatively large volume and narrow impedance and axial ratio bandwidths compared to the proposed antenna. A planar, lightweight, crossed-dipole antenna with CP radiation is introduced for application in a UHF RFID handheld reader in [15], and a CP monopole antenna using a short-circuited sleeve strip for a UHF RFID reader is presented in [16]; both designs have small sizes and printed on a single layer of ground plane. Nevertheless, both antennas have a narrow axial ratio bandwidth and low measured gain, and do not cover the global UHF RFID frequency range.

In this study, we propose a novel low-profile CP reader antenna printed on a low-cost FR-4 material that has a small size and covers the entire UHF RFID band easily. The antenna consists of a CPW L-shaped feedline mounted at the right edge of the square slot at the bottom of the ground plane; a horizontal stub protrudes from the right side of the square slot towards the slot centre, and a vertical stub is placed at the lower left of the square slot. The proposed antenna designed as a universal UHF RFID handheld reader with good peak gain, wider impedance and AR bandwidths, good impedance matching, and compact size. Meanwhile, the antenna has a simple configuration, a planar single-layer ground plane structure, and simple fabrication process.

Details of the proposed universal UHF RFID reader antenna design are described, and a comparison between the simulation and experimental results in terms of reflection coefficient $|S_{11}|$ bandwidth, AR bandwidth, peak gain, and radiation pattern is presented and discussed as well. A parametric study for the significant parameters of the designed antenna as well as a comparison between the proposed antenna and other antennas operating in the UHF RFID band is also conducted.

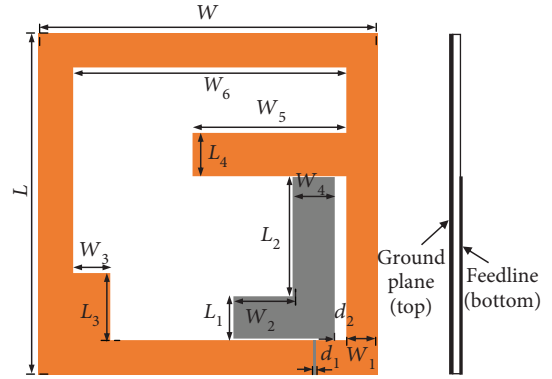


FIGURE 1: Geometry of the proposed antenna.

TABLE 1: Optimal dimensions of the proposed antenna.

Parameter	Value	Parameter	Value	Parameter	Value
L	120	W	120	W_5	54
L_1	16	W_1	11	W_6	96
L_2	42	W_2	21	d_1	1.2
L_3	24	W_3	13	d_2	3.5
L_4	15	W_4	15		

2. Antenna Configuration

The configuration of the proposed compact slot antenna with its dimension is shown in Figure 1. The proposed antenna is fed via a SMA connector by a CPW feedline at the bottom side of the FR4 substrate (loss tangent $\delta = 0.02$, relative permittivity $\epsilon_r = 4.4$, and substrate thickness of 1.6 mm). The CPW feed has a signal strip line with a width of 1.2 mm. One end of the signal strip line was connected to the inverted L-shaped feedline, whereas the other end was connected to a coaxial SMA connector. A wide square slot of $96 \times 96 \text{ mm}^2$ is extracted from the basic square slot on the top side of the ground plane. An inverted L-shaped feedline is mounted on the right side of the lower ground plane to realize the CP characteristic. The proposed antenna has an overall size of $120 \times 120 \text{ mm}^2$. The optimal dimensions of the proposed antenna are listed in Table 1.

The CP characteristic can be realized when two orthogonal E vectors (the complex voltage in the horizontal (E_{Hor}) and vertical (E_{Ver}) plane) of equal amplitude are excited with a phase difference of 90° [17]. To clarify the CP performance of the proposed antenna, Figure 2 demonstrates the evolutionary steps of the proposed antenna and Figure 3 shows the simulation results of the impedance and AR bandwidths for Antennas 1-4. There are four stages (Antenna 1, Antenna 2, Antenna 3, and Antenna 4) when designing an antenna to achieve the proposed antenna. In this article, Antenna 4 is the final design for the proposed antenna. Firstly, Antenna 1 consists of a wide rectangular slot in the ground plane with a CPW inverted L-shaped feedline at the centre of the slot towards the $-y$ axis direction. The L-shaped feedline was used to generate more than one

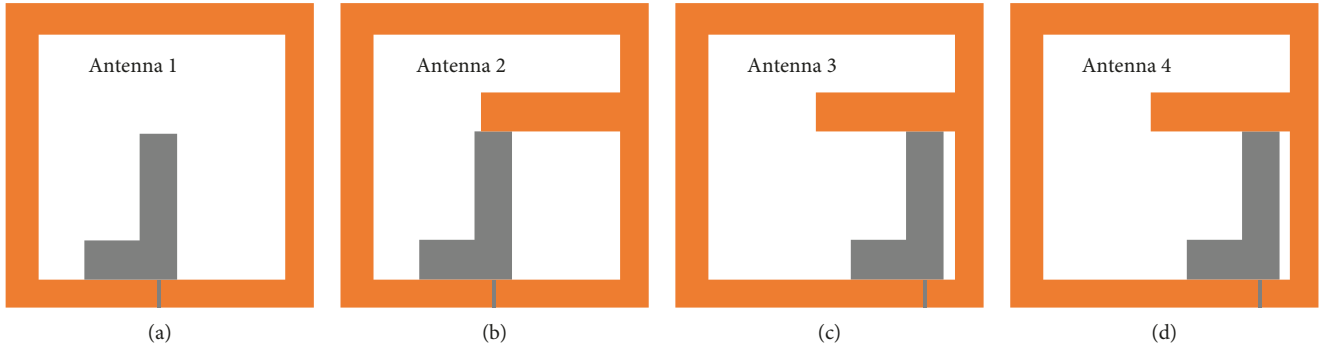
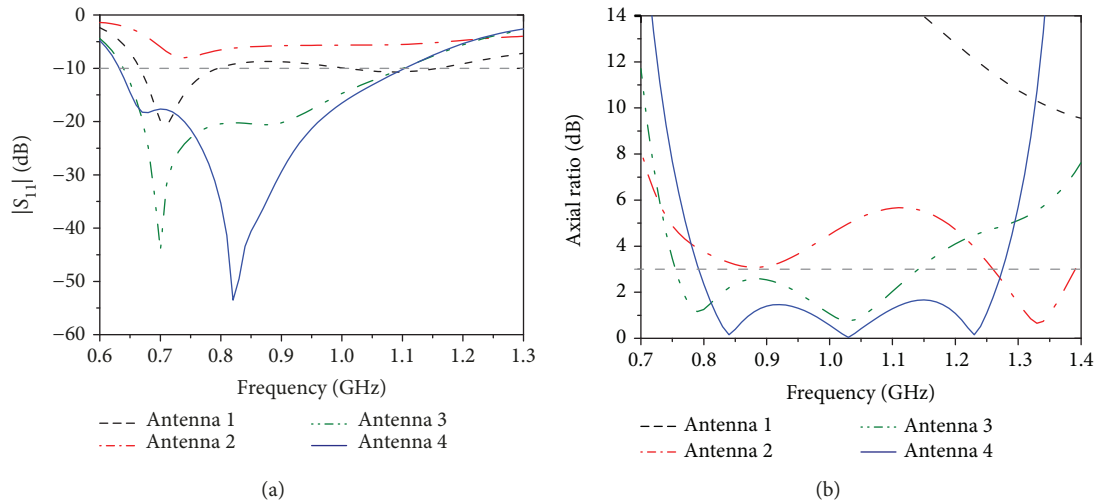


FIGURE 2: Evolutionary steps of the proposed antenna.

FIGURE 3: Simulated (a) S_{11} bandwidth and (b) AR bandwidth results for Antennas 1-4.

resonant frequency. Although Antenna 1 is linearly polarized (with an AR bandwidth around 9 dB), Antenna 1 has a wide impedance bandwidth, as shown in Figure 3. Then, a horizontal stub (along the $-y$ axis) protruded at the right side of the slot toward the slot centre to achieve Antenna 2. Because the E_{Hor} of the horizontal stub ($L_4 \times W_5$) and E_{Ver} of the inverted L-shaped feedline have a 90° phase difference, a broadband CP wave was realized. Although the impedance bandwidth of Antenna 2 was distorted at higher than -10 dB, the CP performance is much better. As shown in Figure 3(b), the simulated 3 dB AR bandwidth is out of the UHF RFID range. In the third stage, to adjust the CP bandwidth on the desired band (UHF RFID band from 840 MHz to 960 MHz) as well as improve the impedance bandwidth significantly, the inverted L-shaped feedline is shifted carefully to the right edge of the rectangular slot underneath the protruding vertical stub to obtain Antenna 3. The results of this stage are a good impedance bandwidth characteristic (from 638 MHz to 1102 MHz) and good 3 dB axial ratio bandwidth (from 755 MHz to 1143 MHz) which easily covered the entire UHF RFID band. Finally, to achieve additional improvement to the antenna performance as a whole, a vertical stub ($L_3 \times W_4$) was added to the structure at the lower left of the square slot, as shown in Antenna 4 (proposed antenna). Antenna 4 shows an impedance bandwidth

characteristic of 472 MHz (632–1104 MHz) and AR bandwidth of 484 MHz (792–1276 MHz).

To investigate the CP behaviour, the surface current distributions at 900 MHz on the square slot and the L-shaped feedline are depicted in Figure 4, illustrating the current direction behaviour at different phases of 0° , 90° , 180° , and 270° . With reference to Figure 4, it is observed that the current distributions on the inverted L-shaped feedline and the square slot are travels in the clockwise direction as the phase angle increases by 90° , exciting a left-hand circularly polarized (LHCP) radiation.

3. Parametric Studies

Parametric studies are conducted to provide additional detailed information about the antenna designing and optimization process. Due to a good agreement between the simulation and measurement results for all antenna parameters, the parametric study is carried out by simulation results as well. The parameters under study include the width of the signal strip line (d_1), the distance between the L-shaped feedline and the right edge of the square slot (d_2), the length of the vertical stub of the L-shaped feedline (L_2), and the length of the horizontal stub (W_5). To understand the influence of these parameters on the performance of the proposed

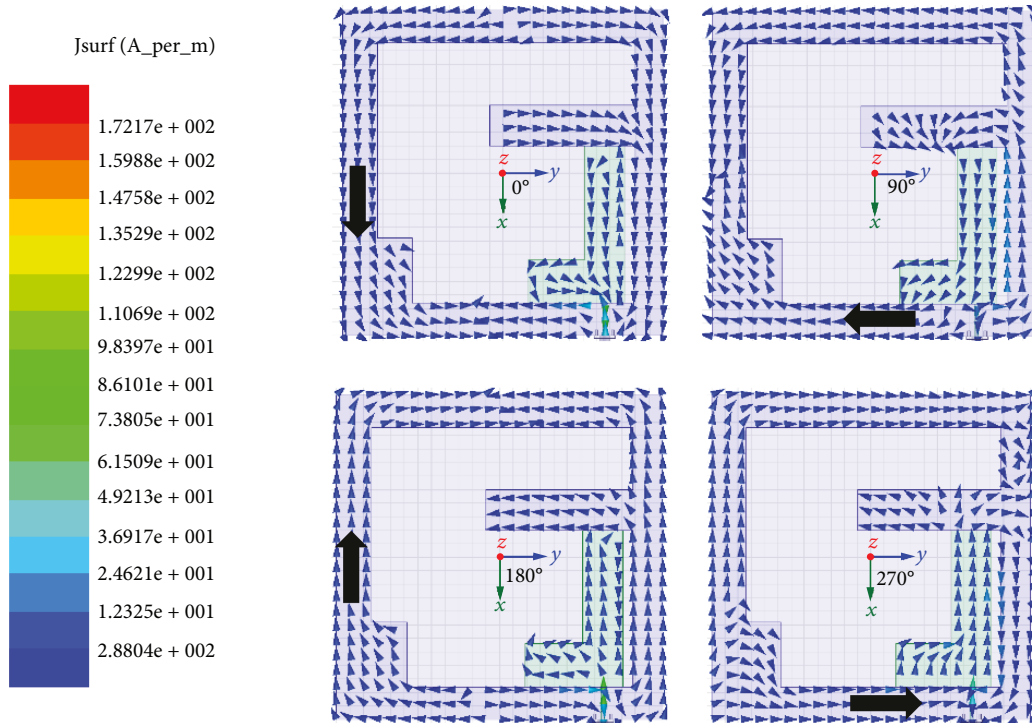


FIGURE 4: Distribution currents of Antenna 4 at 900 MHz.

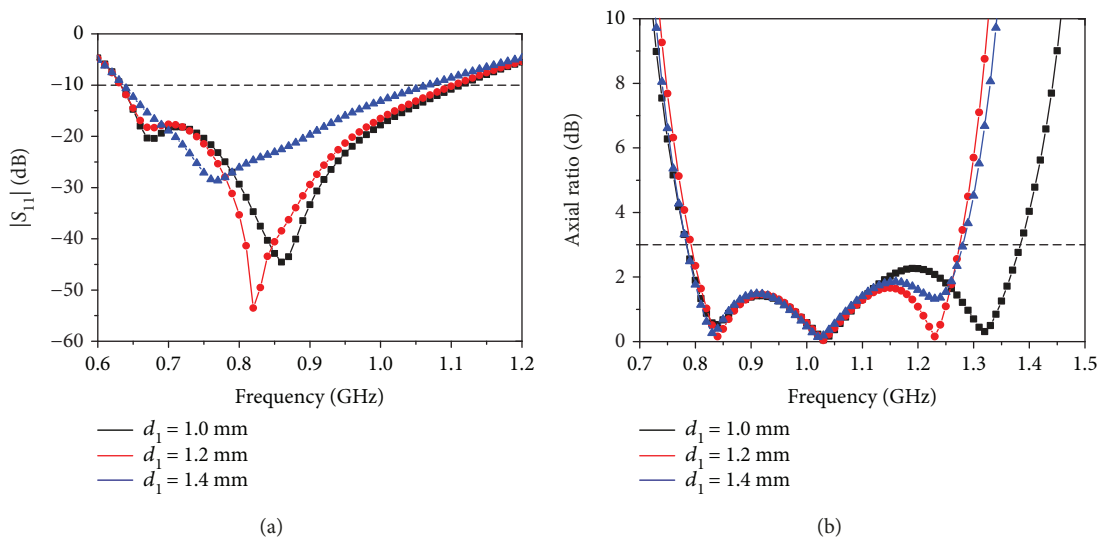


FIGURE 5: Simulated $|S_{11}|$ and AR results for different signal strip widths (d_1).

antenna, only one parameter will be varied, while the other parameters will be fixed.

3.1. Effects of the Width of the Signal Strip Line d_1 . The influence of the width of the signal strip line (d_1) on the performance of the antenna is illustrated in Figure 5. It is found that the value of d_1 just changes the resonant frequency and the impedance matching of the antenna reflection coefficient, but it does not change the start and end bands of the reflection coefficient bandwidth considerably. With reference to the influence of d_1 on the axial ratio bandwidth, it is found

that d_1 changes the axial ratio bandwidth but widens it only when $d_1 = 1.0$ mm.

3.2. Effects of the Parameter d_2 . Figure 6 shows the effect of the distance between the L-shaped feedline and the right edge of the square slot (d_2) on the performance of the antenna. With reference to Figure 6(a), it can be inferred that the resonant frequency of the reflection coefficient bandwidth is increased when the value of d_2 increased. The study shows that the axial ratio bandwidth shifted slightly to lower frequencies when $d_2 = 2.5$ mm and 3.5 mm, and the wider axial

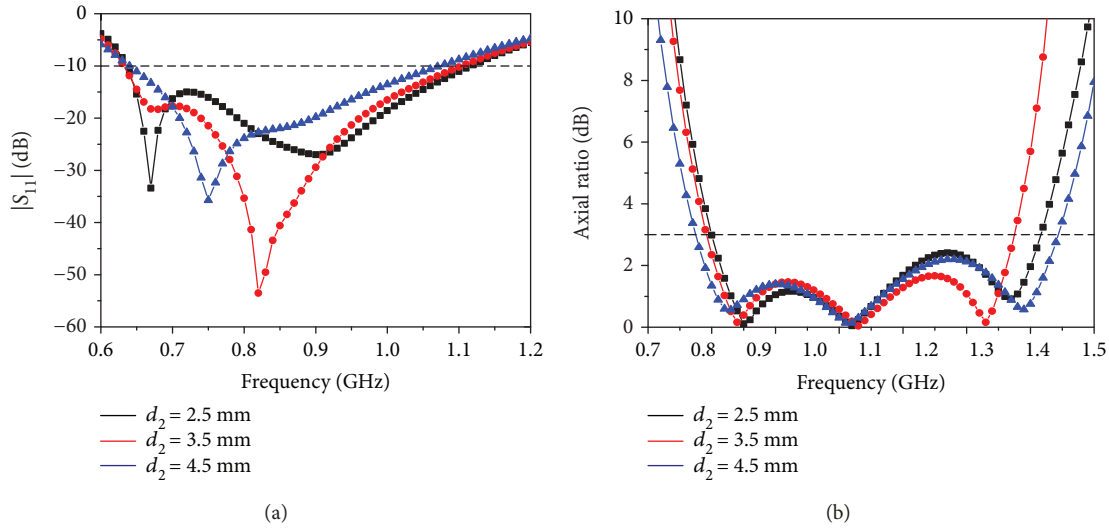


FIGURE 6: Simulated $|S_{11}|$ and AR results for different distances (d_2).

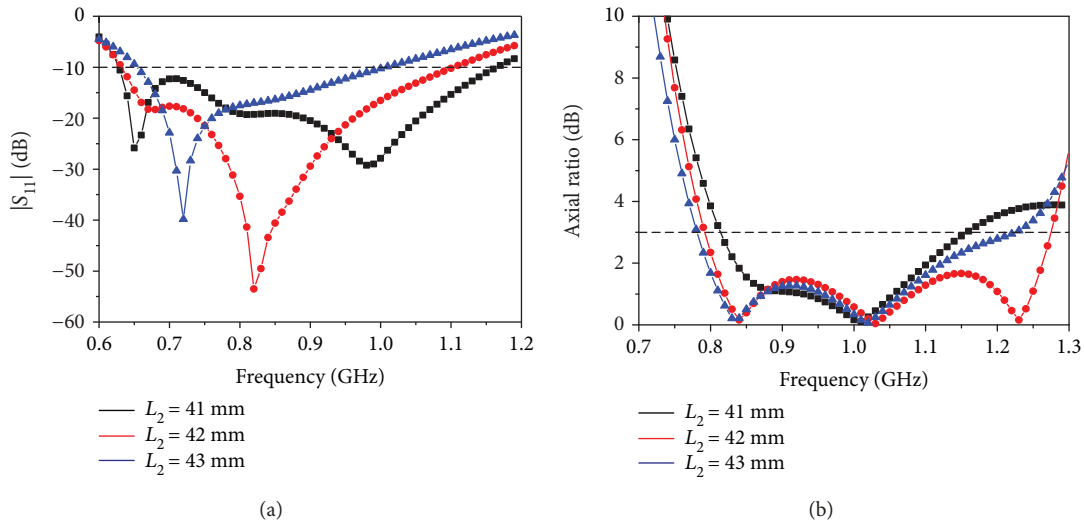


FIGURE 7: Simulated $|S_{11}|$ and AR results for different lengths of the L_2 parameter.

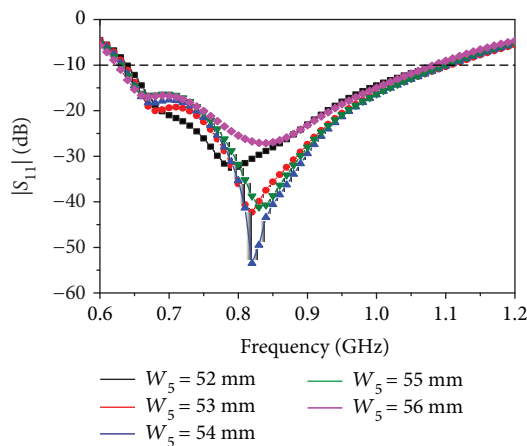


FIGURE 8: Simulated $|S_{11}|$ for different lengths of the horizontal stub (W_5).

ratio bandwidth was achieved at $d_2 = 4.5$ mm, as shown in Figure 6(b).

3.3. Influence of the Length L_2 . The effects of tuning the length of the vertical stub of the L-shaped feedline (L_2) from 41 mm to 43 mm on the $|S_{11}|$ and AR bandwidths are illustrated in Figure 7. As clearly seen in Figure 7(a), the impedance matching and resonance frequency of the reflection coefficient bandwidth increased with the increase in the length of L_2 . The effect of tuning the length (L_2) on the AR bandwidth is demonstrated in Figure 7(b). Although the effect of tuning the length (L_2) from 41 mm to 43 mm on the start frequency of the AR band is inconsiderable, the end frequency of the band is increased as the length of L_2 increased.

It is worth noting that both the impedance matching and resonant frequency of the antenna reflection coefficient $|S_{11}|$ as well as the AR bandwidth can be controlled by tuning the parameter L_2 .

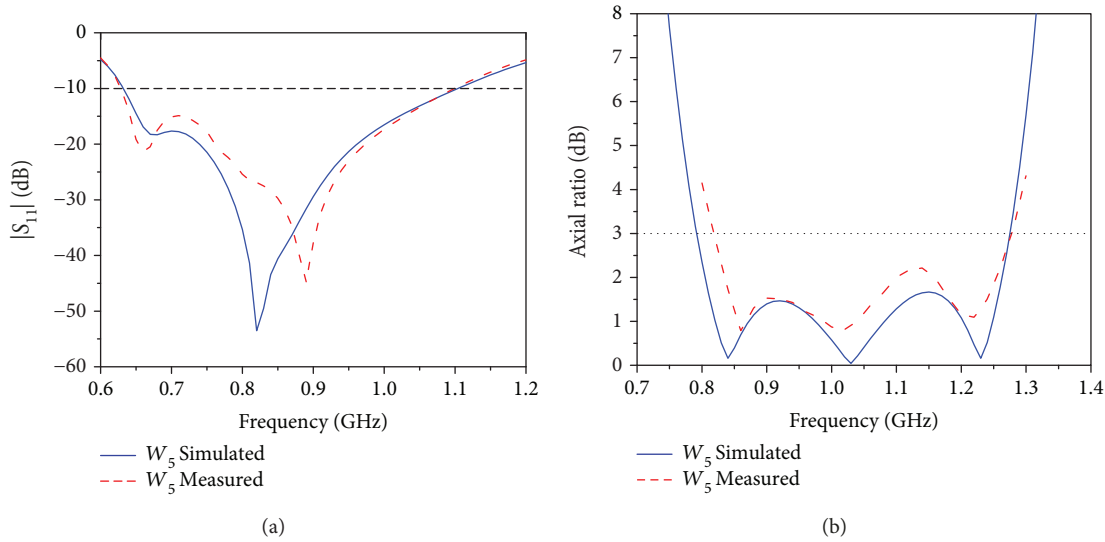


FIGURE 9: Measured and simulated (a) S_{11} and (b) AR results of Antenna 4.

3.4. Impedance Matching Reconfigurability. Figure 8 exhibits the influence of tuning the length of the vertical stub (W_5) on the performance of the antenna reflection coefficient. The increase of W_5 from 52 mm to 54 mm improves the impedance matching of the antenna, as shown in Figure 8. However, when W_5 increased to 55 mm and 56 mm, the antenna impedance matching is decreased. To achieve the optimal performance of the proposed antenna, the value of the length of W_5 is adjusted carefully.

4. Simulation and Measurement Results

An Agilent E5071C vector network analyzer was used to measure the antenna reflection coefficient $|S_{11}|$. The far-field performance of the proposed antenna was measured in an anechoic chamber by using the SATIMO measurement system. The measured and simulated reflection coefficient $|S_{11}|$ results of the proposed compact antenna are demonstrated in Figure 9(a). As shown in the figure, the wide frequency range of both the simulated and measured 10 dB reflection coefficient $|S_{11}|$ bandwidths of 54.4% (632–1104 MHz) and 54.6% (630–1103 MHz) was achieved, respectively. Figure 9(b) presents the simulated and measured results of the axial ratio bandwidth. Wide simulated and measured axial ratio bandwidths of 484 MHz (792–1276 MHz) and 460 MHz (818–1278 MHz) were achieved, respectively. The three CP frequencies (with the lowest AR value) were measured at 840 MHz, 1030 MHz, and 1230 MHz. As a result of integrating these three CP frequencies, a wide broadband CP bandwidth of 42.4% (818–1278 MHz) was measured. Good agreement was observed between the simulated and measured results of the reflection coefficient $|S_{11}|$ and axial ratio bandwidths. As shown in Figure 10, the simulated and measured peak gains of the proposed compact antenna were measured in an authorized SATIMO anechoic chamber, and stable gain levels with small variations of 3.65–4.0 dBi throughout the UHF RFID band (840–960 MHz) can be observed. The

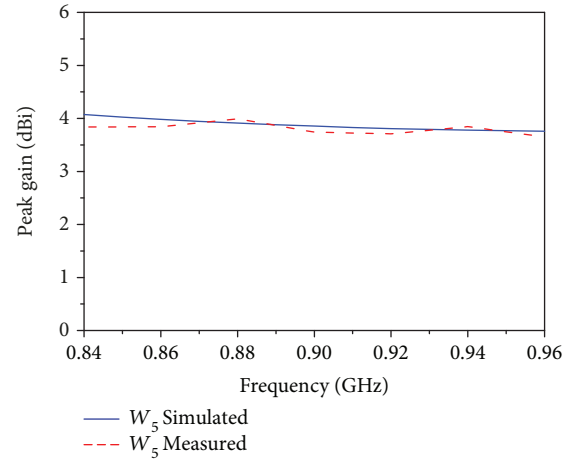


FIGURE 10: Simulated and measured peak gains of the proposed antenna.

maximum measured peak gain of the antenna was at 880 MHz. The normalized simulated and measured radiation patterns in both x - z and y - z planes at 900 MHz (centre frequency of the universal UHF RFID band) are presented in Figure 11, and good agreements between them were observed.

The reading-range measurement of the proposed novel compact CP antenna which was accomplished by rotating the Alien dipole-like tag AZ9662 with dimensions of 70 mm \times 17 mm along the $\pm z$ -axis direction is depicted in Figure 12. The proposed reader antenna was connected to a UHF RFID reader module (JRM2030) with a low output power of 27 dBm and an operating frequency of 902–928 MHz. The antenna exhibited a maximum measured reading range in free space which is maintained between 3.0 and 3.5 meters.

Photographs of the fabricated antenna experiment using the Agilent E5071C vector network analyzer and the SATIMO measurement system are depicted in Figures 13(a) and 13(b),

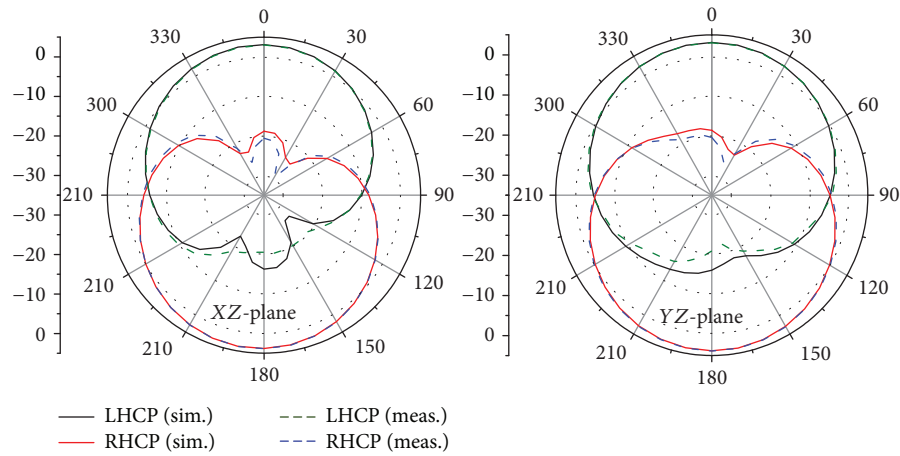


FIGURE 11: Simulated and measured radiation patterns at 900 MHz.

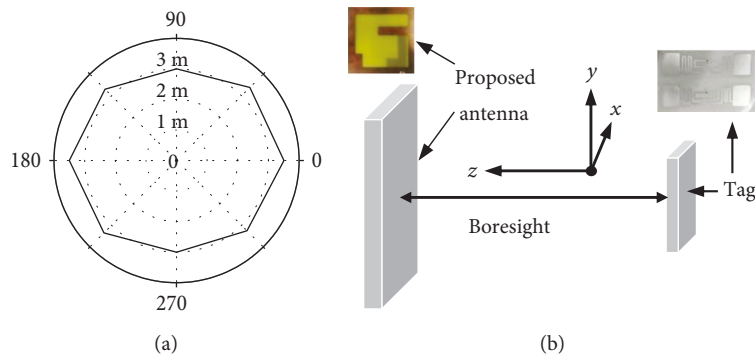


FIGURE 12: Measured reading ranges for the tag rotating in the $\pm z$ -axis.

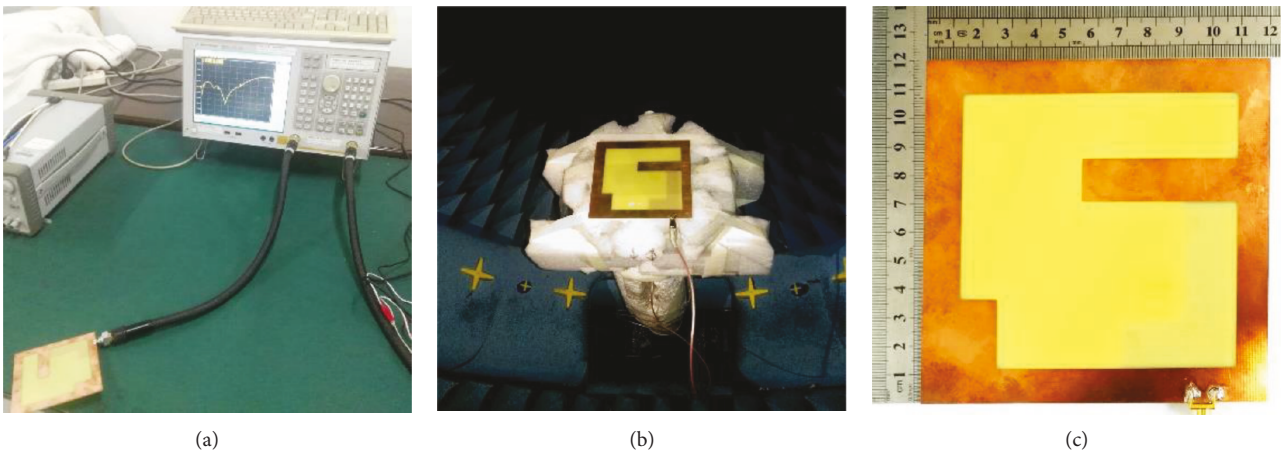


FIGURE 13: Fabricated antenna experiment using (a) the E5071C VNA and (b) the SATIMO measurement system. (c) Photograph of the proposed antenna.

respectively. Figure 13(c) shows a photograph of the fabricated antenna. Table 2 exhibits a comparison between the proposed antenna and the antennas which were designed in references [8–14]. As clearly seen in this table, the overall size of the proposed antenna is small, the CP bandwidth is much wider, and the impedance bandwidth of the proposed antenna is much wider compared to all antennas presented in Table 2. The

proposed antenna is composed of one ground plane layer, while the antennas in [8–11] consisted of more than one ground plane layer. Notably, the proposed universal UHF RFID antennas covered the entire UHF RFID band of 840–960 MHz in terms of impedance and axial ratio bandwidths, whereas the antennas in [8–10, 12, 13, 15, 16] cannot be considered as a universal antenna type (840–960 MHz).

TABLE 2: Comparison between the proposed antenna and other CP reader antennas.

Ant.	-10 dB $ S_{11} $ BW (MHz/%)	3 dB AR BW (MHz/%)	Max. gain (dBi)	Sizes ($L \times W \times H$) (mm ³)	No. of layers
[8]	140 835-975	70 870-940	5.0	124 × 117 × 33.2	2
[9]	194 768-962	141 816-957	9.8	250 × 250 × 35	4
[10]	220 880-1100	29 901-930	7.3	150 × 150 × 34	2
[11]	180 800-980	180 820-1000	6.5	250 × 250 × 17.3	4
[12]	225 758-983	121 838-959	8.6	250 × 250 × 36.5	4
[13]	142 860-1002	166 857-1023	6.8	126 × 121 × 0.8	1
[14]	380 618-998	332 791-1123	3.4	120 × 120 × 0.8	1
[15]	90 851-941	19 902-921	1.4	60 × 60 × 0.508	1
[16]	185 794-979	60 900-960	1.58	80 × 80 × 1.6	1
Our work	473 630-1103	460 818-1278	4.0	120 × 120 × 1.6	1

5. Conclusion

In this study, a new reader antenna for universal UHF RFID handheld applications was demonstrated and experimentally investigated. The proposed antenna consists of a CPW L-shaped feedline mounted at the right edge of the square slot at the bottom of the ground plane, with a horizontal stub protruding from the right side of the square and a vertical stub placed at the lower left of the square slot. The positions and geometries of these L-shaped feedlines and stubs are carefully adjusted to obtain a wide CP bandwidth. The proposed antenna shows a measured impedance bandwidth of 54.6% (630–1103 MHz) with a reflection coefficient less than -10 dB, a 3 dB axial ratio bandwidth of 460 MHz (818–1278 MHz), and a stable radiation gain between 3.65 and 4.0 dBi throughout the universal UHF RFID band (840–960 MHz). The proposed antenna has the merits of compact size, simple structure, easy fabrication process, and wide axial ratio bandwidth compared to the reader antennas mentioned in Table 2. The measured antenna performances mentioned above indicate that the proposed antenna easily satisfies the requirements of the universal UHF RFID handheld reader antenna applications with a wide axial ratio bandwidth and a compact overall size of only $120 \times 120 \times 1.6 \text{ mm}^3$.

Data Availability

The simulated and measured results for each parameter are plotted in one figure as a comparison between the simulation and measurement results.

Conflicts of Interest

The authors declare that there is no conflict of interest regarding the publication of this paper.

Acknowledgments

This work is supported by the Key Project of the National Natural Science Foundation of China under Grants 61531016 and 61831017 and the Sichuan Provincial Science and Technology Important Projects under Grants 2018GZ0139 and 2018GZDZX0001.

References

- [1] A. Ren, C. Wu, Y. Gao, and Y. Yuan, "A robust UHF near-field RFID reader antenna," *IEEE Transactions on Antennas and Propagation*, vol. 60, no. 4, pp. 1690–1697, 2012.
- [2] J. K. Pakkathillam, M. Kanagasabai, and M. G. N. Alsath, "Compact multiservice UHF RFID reader antenna for near-field and far-field operations," *IEEE Antennas and Wireless Propagation Letters*, vol. 16, pp. 149–152, 2017.
- [3] Q. Liu, J. Shen, J. Yin, H. Liu, and Y. Liu, "Compact 0.92/2.45-GHz dual-band directional circularly polarized microstrip antenna for handheld RFID reader applications," *IEEE Transactions on Antennas and Propagation*, vol. 63, no. 9, pp. 3849–3856, 2015.
- [4] T. Wu, H. Su, L. Gan, H. Chen, J. Huang, and H. Zhang, "A compact and broadband microstrip stacked patch antenna with circular polarization for 2.45-GHz mobile RFID reader," *IEEE Antennas and Wireless Propagation Letters*, vol. 12, pp. 623–626, 2013.
- [5] W.-S. Chen and Y.-C. Huang, "A novel CP antenna for UHF RFID handheld reader," *IEEE Antennas and Propagation Magazine*, vol. 55, no. 4, pp. 128–137, 2013.
- [6] M. H. Hoang, T. Q. Van Hoang, H. P. Phan, and T. P. Vuong, "Cavity-backed circular-polarized compact slot antenna for handheld UHF RFID reader," *IEEE Antennas and Wireless Propagation Letters*, vol. 14, pp. 1439–1442, 2015.
- [7] Nasimuddin, Z. N. Chen, and X. Qing, "Asymmetric-circular shaped slotted microstrip antennas for circular polarization and RFID applications," *IEEE Transactions on Antennas and Propagation*, vol. 58, no. 12, pp. 3821–3828, 2010.
- [8] T.-N. Chang and J.-M. Lin, "Circularly polarized ring-patch antenna," *IEEE Antennas and Wireless Propagation Letters*, vol. 11, pp. 26–29, 2012.
- [9] X. Liu, Y. Liu, and M. M. Tentzeris, "A novel circularly polarized antenna with coin-shaped patches and a ring-shaped strip for worldwide UHF RFID applications," *IEEE Antennas and Wireless Propagation Letters*, vol. 14, pp. 707–710, 2015.
- [10] C.-Y.-D. Sim and C.-J. Chi, "A slot loaded circularly polarized patch antenna for UHF RFID reader," *IEEE Transactions on Antennas and Propagation*, vol. 60, no. 10, pp. 4516–4521, 2012.
- [11] H. L. Chung, X. Qing, and Z. N. Chen, "A broadband circularly polarized stacked probe-fed patch antenna for UHF RFID applications," *International Journal of Antennas and Propagation*, vol. 2007, 8 pages, 2007.
- [12] Z. Wang, S. Fang, S. Fu, and S. Jia, "Single-fed broadband circularly polarized stacked patch antenna with horizontally meandered strip for universal UHF RFID applications," *IEEE*

- Transactions on Microwave Theory and Techniques*, vol. 59, no. 4, pp. 1066–1073, 2011.
- [13] J.-H. Lu and S.-F. Wang, “Planar broadband circularly polarized antenna with square slot for UHF RFID reader,” *IEEE Transactions on Antennas and Propagation*, vol. 61, no. 1, pp. 45–53, 2013.
- [14] R. Cao and S.-C. Yu, “Wideband compact CPW-fed circularly polarized antenna for universal UHF RFID reader,” *IEEE Transactions on Antennas and Propagation*, vol. 63, no. 9, pp. 4148–4151, 2015.
- [15] S. X. Ta, H. Choo, and I. Park, “Planar, lightweight, circularly polarized crossed dipole antenna for handheld UHF RFID reader,” *Microwave and Optical Technology Letters*, vol. 55, no. 8, pp. 1874–1878, 2013.
- [16] C.-Y. Pan, C.-C. Su, G.-J. Wu, and J.-Y. Jan, “Circularly polarized monopole antenna using short-circuited sleeve strip for UHF RFID reader,” *Microwave and Optical Technology Letters*, vol. 56, no. 4, pp. 957–961, 2014.
- [17] M. S. Ellis, Z. Zhao, J. Wu, X. Ding, Z. Nie, and Q.-H. Liu, “A novel simple and compact microstrip-fed circularly polarized wide slot antenna with wide axial ratio bandwidth for C-band applications,” *IEEE Transactions on Antennas and Propagation*, vol. 64, no. 4, pp. 1552–1555, 2016.



Hindawi

Submit your manuscripts at
www.hindawi.com

